Dynamic Modeling and Self-Optimizing Control of Air-Side Economizers

Pengfei Li and Yaoyu Li

Department of Mechanical Engineering
University of Wisconsin – Milwaukee
pli@uwm.edu & yyli@uwm.edu

John E. Seem

Building Efficiency Research Group
Johnson Controls, Inc.
john.seem@gmail.com

Abstract

For the heating, ventilating, and air conditioning (HVAC) systems for commercial buildings, there has been a greater demand for reducing energy consumption. The economizers have been developed as a class of energy saving devices that may increase the energy efficiency by taking advantage of outdoor air during cool or cold weather. However, in practice, many economizers do not operate in the expected manner and waste even more energy than before installation. Better control strategy is needed for optimal and robust operation. This paper presents two related aspects of research on dynamic modeling and control for economizers. First, a Modelica based dynamic model is developed for a single-duct air-side economizer. The model development was based on Dymola and AirConditioning Library with some revision on water medium and heat exchanger modeling. Such transient model will lay a more quality foundation for control design. Second, for a three-state operation for air-side economizers, a self-optimizing control strategy is developed based on the extremum seeking control (ESC). The mechanical cooling can be minimized by optimizing the outdoor air damper opening via extremum seeking. Such has much less dependency on the knowledge of economizer model, and thus has more promise for practical operation. In addition, an anti-windup ESC scheme is proposed as an enhancement for the existing ESC techniques. The simulation results validated the effectiveness of the dynamic model of the economizer, demonstrated the potential of using ESC to achieve the minimal mechanical cooling load in a self-optimizing manner, and illustrated the possibility of ESC malfunctioning under actuator (damper) saturation and the capability of anti-windup ESC in preventing such undesirable behavior.

Keywords: *Modelica; transient modeling; economizer; extremum-seeking control*

1 Introduction

Buildings are responsible for a large portion of electricity and natural gas demand. Significant amount of energy consumption for buildings is due to the heating, ventilation and air conditioning (HVAC) systems. Improving the efficiency of building HVAC system is thus critical for energy and environmental sustainability. The economizers have been developed as a class of energy saving devices that may increase the energy efficiency by taking advantage of outdoor air during cool or cold weather [1]. Figure 1 is a schematic diagram of a typical single-duct air-handling unit (AHU) and controller. The AHU has a supply fan, three (outdoor air, relief air and mixed air) dampers for controlling air flow between the AHU and the outdoors, heating and cooling coils for conditioning the air, a filter for removing airborne particles, various sensors and actuators, and a controller that receives sensor measurements (inputs) and computes and transmits new control signals (outputs). The air economizer moves the dampers to let in 100% outdoor air when it is cool but not extremely cold outside. When it is hot outside, the dampers are controlled to provide the minimum amount of outdoor air required for ventilation.

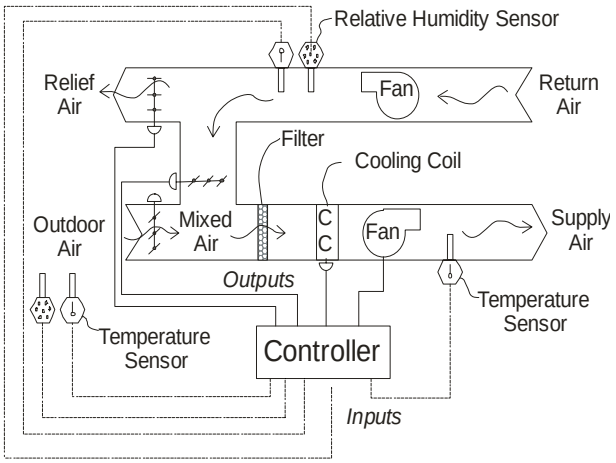

Figure 1: Single duct air handling unit

The American Society of Heating, Refrigerating and Air Conditioning Engineers (ASHRAE) recommends using economizers based on the cooling capacity size and weather characteristics for the building location [2], as described in the Appendix. ASHRAE [3] describes several control strategies for transitioning between 100% outdoor air and the minimum outdoor air required for ventilation. The control strategies are called "high limit shutoff control for air economizer." Following is a list of strategies that can be programmed in a computer control system.

- *Fixed dry bulb temperature*. This strategy compares the outdoor temperature to a transition temperature. If the outdoor air temperature is greater than the transition temperature, then the dampers are controlled for the minimum outdoor air required for ventilation.
- *Differential dry bulb temperature*. This control strategy compares the outdoor and return air temperatures. If the outdoor temperature is greater than the return air temperature, then the dampers are controlled for minimum outdoor air required for ventilation.
- *Fixed enthalpy*. This control strategy measures the outdoor air temperature and relative humidity (RH). Then the outdoor air enthalpy is calculated and compared with a transition enthalpy. If the outdoor air enthalpy is greater than the transition enthalpy, then the dampers are controlled for minimum outdoor air required for ventilation.
- *Differential enthalpy*. This control strategy determines the outdoor and return air enthalpy from measurements of the outdoor and return air temperature and relative humidity. If the outdoor air enthalpy is greater than the return air enthalpy, then the dampers are controlled for minimum outdoor air required for ventilation.

However, in practice, many economizers do not operate as expected and waste even more energy than before installation [4]. Temperature and RH sensor errors can have a large impact on the energy savings or possible penalty of economizer strategies. The National Building Controls Information Program (NBCIP) [5] said, "In the case of economizers, relative humidity and temperature measurements of outdoor and return air conditions are used to calculate the enthalpies of the two air streams. The air stream with the least energy content is then selected to provide building cooling. If one or both of the computed enthalpies is wrong, as can happen when humidity transmitters are not accurate, significant energy penalties can result from cooling of the incorrect air stream." The NBCIP [6] performed long term performance tests on 20 RH sensors from six manufacturers. Nine of the 20 RH sensors failed during the testing. All of the remaining sensors had many measurements outside of specifications. The largest mean error was 10% RH, and the largest standard deviation of the error was 10.2%. The best performing sensor had a mean error of –2.9% RH and a standard deviation of 1.2%. The specifications for the best performing sensor were ±3%. Control strategies not relying on RH measurement would greatly enhance the reliability of economizer operation.

Modeling and optimal control of air-handling units and economizers have been previously studied [7, 8]. However, due to the complex nature of HVAC system operation, the obtained model may not be accurate enough for the optimal operation of an economizer. Therefore, a model based optimal control approach is hardly effective in practice to seek the optimal outdoor air flow for minimizing the mechanical cooling. In contrast, an on-line self-optimizing control approach appears a more suitable option.

This research investigates the application of the extremum seeking control (ESC) [9-13] to optimize the use of outdoor air so as to minimize the energy consumption. The input and output of the proposed ESC framework are the damper opening and power consumption (or equivalently, the chilled water flow rate), respectively. This approach does not rely on the use of relative humidity sensor and accurate model of the economizer for optimal operation. Therefore, it provides a more reliable control strategy for economizer operation. The proposed ESC scheme works as part of a three-state economizer control strategy, as shown in the state diagram in Figure 2. State 1 uses heating to maintain the supply air temperature. In state 2, outside air is mixed with the return air to maintain the supply air at a given setpoint. In state 3, the extremum seeking control is used to control the dampers to minimize the mechanical cooling load. Also, the dampers must be controlled to guarantee enough outdoor air inflow to satisfy the ventilation requirement for the rooms. Figure 3 shows the control regions for different outside air conditions on a psychometric chart. The return air condition was 75 °F and 50% relative humidity, the cooling coil was ideal, and the minimum fraction of outdoor air to supply air was 0.3. The heating region is for state 1, the free cooling region is for state 2, and the three regions that need mechanical cooling are combined into state 3.

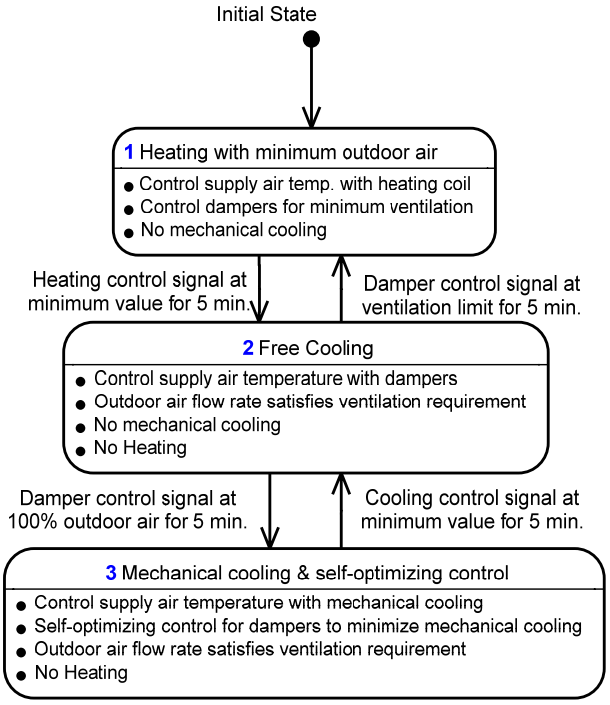

Figure 2: State transition diagram for the proposed control strategy.

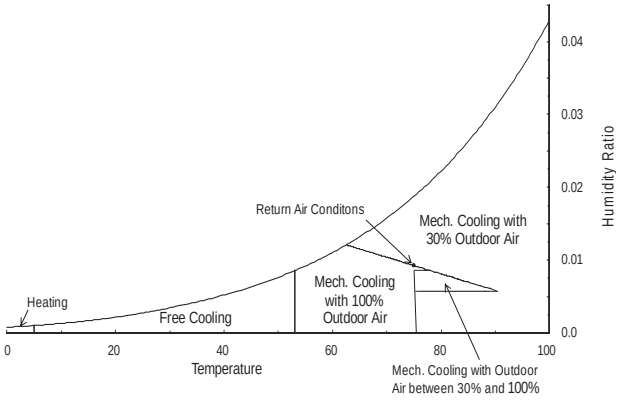

Figure 3: Control states for different outside air conditions for an ideal coil with return conditions 75 °F and 50% RH.

The proposed control scheme has the following advantages over existing economizer strategies:

- *Energy Savings*. Using ESC will lead to energy savings because the dampers will be controlled to minimize the mechanical cooling load. Also, the proposed strategy will save energy because it is not dependent on unreliable RH sensors.
- *Lower installed costs* because the proposed strategy does not require the outside air or return air temperature or RH sensors.
- *Lower maintenance costs* because the temperature and RH sensors do not need to be calibrated.

In addition to the ESC application for economizer control, an enhancement on the ESC is proposed: an anti-windup ESC scheme against damper (actuator) saturation. Due to the inherent integral action incorporated in the ESC loop, the integral windup due to the damper saturation would disable the ESC, as will be shown in Section 3. The back-calculation scheme is applied to the ESC loop to achieve the anti-windup capability.

In order to design and simulation the proposed control strategy, a quality dynamic model of economizer is needed. In this study, an economizer simulation model was developed in Modelica. Dynamic modeling of HVAC equipment has attracted increasing attention in recent years. A summary of previous work in dynamic modeling of vapor compression equipment was presented in [14, 15]. According to [15], the modeling regimes could be mainly classified as two categories: reference models and lumped models. The reference models are designed to best fit the underlying physics of the system, but will often involve partial differential equations (PDE) and high system order. In contrast, the lumped models will lead to lower order ordinary differential equations (ODE) based on some simplifications and/or space discretization. In particular, the first category of models requires extensive dynamic information from the heat exchanger. The finite-volume method was studied by MacArthur [16] but with simplifications in decoupling thermal responses from pressure responses, which may result in less accurate mass distribution predictions. This issue was latter resolved by MacArthur and Grald [17] from combining the mass and balance equations, where the pressure responses are involved. Nyers and Stoyan [18] modeled an evaporator using the approach of finite-difference. Williatzen et al [19] employed a profile assumption for the variation of refrigerant state within each phase region. Recently, Rasmussen [20] presents an novel modeling approach with more freedom of selecting the system states and is claimed to be equivalent to the common method of simplifying the governing PDEs to the desired ODEs. Zhou [21] developed a so-called forward model which was capable of solving the governing differential equations concerning energy storage and transfer in a cooling and dehumidifying coil. The lumped models have also been studied by several authors for simulation and control purposes [22-24]. Besides the modeling approaches involved, the fact that different time scales of the system dynamics are either interwoven or distinctive to a large extent yet poses another serious challenge to the dynamic modeling of HVAC. However, limited study has been done so far

on developing effective and efficient dynamic models that are capable of handling system dynamics with different time scales and simultaneously satisfying research purposes ranging from dynamic analysis and control design of subsystems (e.g. AHU) to building energy savings and comfort. As for AHU modeling in particular, ASHRAE [15] said some of the quickest phenomena occur in the AHUs (coils, humidifiers, and economizers), when simulating such subsystems, realistic dynamics have to be considered for all components involved: heat and mass exchangers, fans, ducts and pipes, sensors and actuators. Compared to the control oriented transient analysis which features small time-scale, the energy saving and human comfort evaluation are coped with in a much larger time scale, but require accurate energy balances. For instance, the cooling coil usually has the slowest transient among the four major components in the vapor compression system, and thus has the largest impact on transient performance. It is necessary to consider mass distribution within the cooling coil as a function of time and space and this requires transient mass balances to allow for local storage [14]. On the other hand, for an AHU, the cooling coil is among the quickest responding components. Their transient response may significantly interact with closed loop controllers [15]. Thus, the multiple-time-scale compatibility is important for the dynamic/transient modeling of HVAC systems.

Control development for many HVAC systems, e.g. the economizer in this study, would not be possible without accurate and computationally efficient dynamic/transient models. Most simulation tools for HVAC systems have been based on steady-state modeling. Dynamic modeling and simulation is still in the research phase and not mature yet. Modelica, as an object-oriented language for physical modeling, has demonstrated its great capability for simulating multi-physical systems. Several Modelica based simulation packages have been developed, e.g. the Thermal-Fluid Library [25], the AirConditioning Library [26], the Modelica_Fluid Library [25] and the HITLib [27]. The AirConditioning Library is capable of handling both steady-state and transient simulation, however, it was mainly designed for automotive air conditioning systems. Some components need to be modified for modeling building HVAC systems such as economizers. In this study, a dynamic model of a single-duct air-side economizer is developed using Dymola (Version 6.1) developed by Dynasim [28], the Modelica Fluid Library (MFL) and the AirConditioning Library (ACL) (Versions 1.4 and 1.5) developed by Modelon [26].

The remainder of this paper is organized as follows. Section 2 describes the dynamic economizer model design. The details of ESC design are described in Section 3, along with the anti-windup ESC. Finally, simulation results that demonstrate the effectiveness of ESC and the two proposed enhancements are presented in Section 4.

2 Dynamic Economizer Model Design

The dynamic model of economizer was developed based on the Dymola 6.1, the MFL and the ACL 1.4 and 1.5. In addition to adopting the standard components in the commercial packages, we have made the following development: modification of water property calculation for the heat exchanger model, initialization with pressure-temperature pair, mixing box, and fan. Figure 4 shows the economizer model that we have developed in Dymola, which includes air ducts, air mixing box, fans, cooling coil, and a room space. The air duct model was adopted from the MFL. It allows detailed pressure drop calculation due to wall friction. The air mixing box model contains two sub-components: the air-mixing plenum and the damper module. The air-mixing plenum was developed using the splitter model from the MFL, while the damper module was developed by ourselves. We have also developed a fan model based on the similarity factors [29]. In addition, the cooling coil was developed based on the evaporator model from the ACL. A water medium model *CoolWater* was developed based on the IAWSP-IF97 formulation [30], and compared with the water medium model developed in the ACL. The pressure-temperature pair was used for both initialization and state derivation with the consideration of practical HVAC operation. Finally, a mixing volume model from the MFL was used to represent a room space.

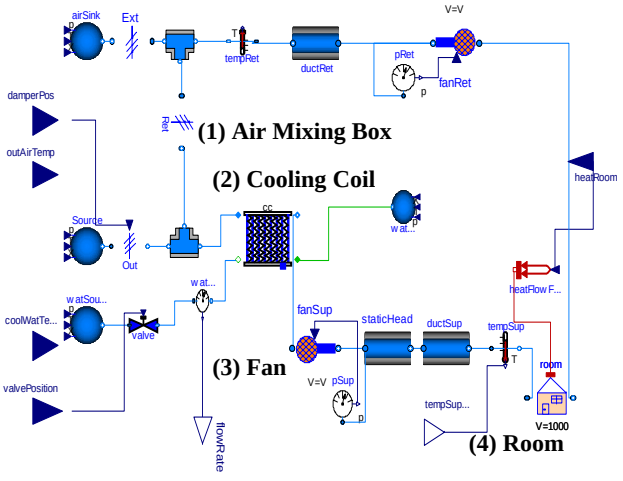

Figure 4: Dymola layout of the economizer model.

2.1 Air Mixing Box

The air mixing box is a component of the AHU that mixes the outdoor air and the return air from the conditioned indoor space. It consists of a damper module (outdoor, return and exhaust dampers) and an air-mixing plenum. The fraction of the outside air is regulated by the outdoor damper whose command signal is interlocked with the exhaust and return air damper. The supply air flow rate is kept as consistent as possible to ensure proper pressure balance at the building side. In addition, to provide adequate ventilation, the minimal OAD opening is limited by an actuator. The damper model was developed based on the work by Tan and Dexter [31]. The pressure drop across the dampers is given by $P_{loss} = R_{damp} m_{air}^2$, where m_{air} is the mass flow rate of the air through the dampers and R_{damp} is the resistance of the damper given by

$$R_{damp} = \begin{cases} R_{open} \exp[k_d(1-\alpha)] & \text{if } \alpha \geq 0.3333 \\ \dfrac{R_{open}}{3.0[(1/3-\alpha)L_d + 0.0429\alpha]^2} & \text{if } \alpha < 0.3333 \end{cases} \quad (1)$$

where α is the fractional opening of the damper (0 for fully closed and 1 for fully open), k_d is a constant depending on the type of blades used, R_{open} is the resistance of fully open dampers, and L_d is the leakage when the damper is fully closed. In Eq. (1), there exists a slight discontinuity of the damper resistance around 0.3333. It was smoothed by a third order polynomial covering the interval of [0.2833, 0.3833]. The four coefficients of the polynomial were determined with the two functional values and two derivative values at 0.2833 and 0.3833. The air-mixing plenum was formulated on the basis of the splitter model from the MFL.

2.2 Fan

Two fan models are employed in this study. The first fan model was based on the pump model from the MFL. The only change was on the medium flowing through, from water to the moist air. The second fan model was developed based on the similarity factor model in [29]. The relationship between the flow factor and pressure factor is given by

$$\varphi = C_1 + C_2\psi + C_3\psi^2 \quad (2a)$$

$$\varphi = \frac{Q}{AU} \quad (2b)$$

$$\psi = \frac{\Delta P_{total}}{\Delta P_{dynam,\ periph}} \quad (2c)$$

where $A = (\pi D^2)/4$, $U = (\pi DN)/60$, $\Delta P_{vel} = (\rho v^2)/2$, $v = Q / A_{ex}$, $\Delta P_{total} = \Delta P_{stat} + \Delta P_{vel}$, φ is the flow factor, ψ is the pressure factor, Q is the flow rate, A is the reference area, A_{ex} is the exhaust area, D is diameter of the impeller, v is the velocity of the outflow air, N is the rotation speed in rpm, ΔP_{stat} is the static pressure, ΔP_{vel} is the velocity pressure, and $\Delta P_{dynam,\ periph}$ is the peripheral dynamic pressure. C_1, C_2 and C_3 are coefficients of the polynomials relating the flow and pressure factors, which are fitted to the manufacture's fan performance data by the least-square estimation. A limited proportional-integral (PI) controller is used to regulate the rotation speed of the supply fan to maintain the static pressure of the supply air duct at the setpoint. In addition, the rotation speed of the return fan is synchronized by another limited PI controller, with the reference setting satisfying the steady-state equilibrium of overall flow rate. This is a simplified treatment, and it is being improved by a more accurate treatment described in the work by Tan and Dexter in [31] which considered the building over-pressurization and leakage flow.

2.3 Cooling Coil

Cooling coil is the most important component between the primary plant (e.g. chiller) and the air distribution system. As mentioned earlier, the cooling coil is among the quickest responding components in AHU and it also responds to the quickest perturbations. Therefore, the transient behavior of cooling coil may have significant effect on closed loop control performance [15].

Since Version 1.4, the ACL has developed a group of heat exchanger models that are capable of simulating both transient and steady-state operations. The dynamic energy and mass balances are formulated based on the finite-volume method. The number of discretization at the refrigerant side is proportional to that for the solid wall and the air side. The heat conduction in the solid wall is modeled as a one-dimensional problem perpendicular to the fluid flow direction. In particular, the simulation results of a cross-counter flow evaporator model used in an automotive R134a-system had been validated in an experiment conducted by Chrysler [32]. The measured data were compared with the simulation results of the medium properties and the steady-state heat transfer rates, for three sets of boundary conditions given by the mass flow rate, the inlet temperature, the inlet enthalpy, and the relative humidity of the ambient air. The heat transfer rates had good consistency while the refrigerant-side pressure drop and the air-side water condensing needed improvement.

There were some challenges to directly use the heat exchanger model from ACL for the cooling coil component in the economizer model. In the ACL Version 1.5, the choices of state variable pairs include pressure-enthalpy, density-temperature, and mass-internal energy. Such choices are suitable for the air flow and two-phase refrigerants in the automotive refrigeration systems. However, for the building HVAC systems, especially for cooling coils in the AHU, the working medium is typically single-phase, i.e. water. Also, the temperature range is limited to the ambient temperature variation. Therefore, it is necessary to reformulate the existing heat exchanger model in the ACL to accommodate the specific needs in building HVAC systems.

2.3.1 Medium Model Design and Implementation

An accurate water medium model is critical for the transient simulation of cooling and heating coils in the AHU. For the water property calculation, there are mainly two international standard formulations, namely, IAPWS95 [33] and IAPWS-IF97 [30, 33]. The former was developed for scientific computation, while the latter was developed for industrial applications. Prior to the release of Version 1.4, the ACL had included a large set of medium models for many refrigerants, but not the water medium. Since Version 1.5, the ACL has adopted a lookup-table (LUT) based incompressible fluid (water) medium model for heat exchanger modeling. However, it may have the following drawbacks. First, in the control volumes, pressure responses are decoupled with thermal responses, which may lead to inaccurate mass distribution predictions. Second, incompressible water model will also result in inaccurate pressure drop calculations, which will in turn affect the heat transfer property calculations.

To validate the accuracy of different formulations of water property model, the IF-97 formulae based model (abbreviated as "IF-97 model" later) and the LUT based incompressible water model (abbreviated as LUT model later) were compared with the IAPWS-95 standard. The FLUIDCAL program developed by Wagner's group was used to obtain the IAPWS-95 based water properties [34]. For Dymola 6.1, the water medium in Modelica_Media follows the IF-97 model, while the water medium of ThermoFluidPro in the ACL Version1.5 follows the LUT model. The comparison was conducted in the temperature range from 274.15 K to 373.15 K with an increment of 5 K, and the pressure input was set 5 bars for all cases. Table 1 summarizes the maximum errors of several properties based on the IF-97 and LUT models relative to those derived from the IAPWS-95 standard. Figures 5 through 8 compare the relative errors of the IF-97 and LUT models in density, specific entropy, C_p and C_v, respectively. Note that C_p and C_v are assumed identical in the LUT model. More discrepancies were observed for entropy and C_v.

Table 1: Water Properties Based on IF-97 and LUT Models Relative to IAPWS-95 Standard

Water Property	Maximum Relative Error (%)	
	IF-97	ACL1.5
Density	0.0015	0.09
Specific Entropy	0.018	28.223
C_p	0.052	0.189
C_v	0.075	11.833

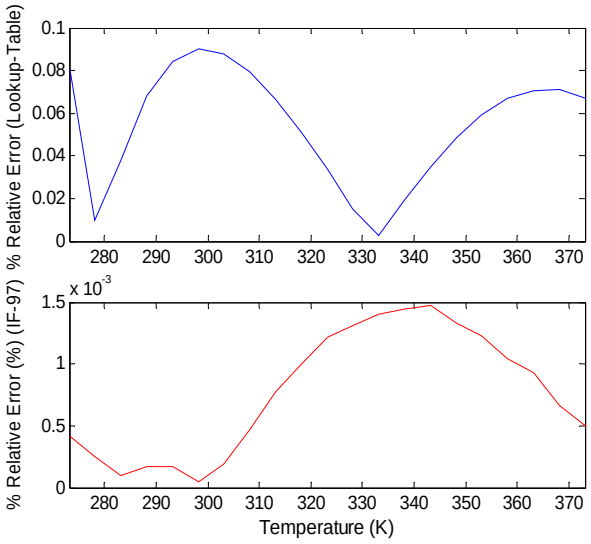

Figure 5: Density errors of the IF-97 and LUT models relative to the IAPWS95 standard

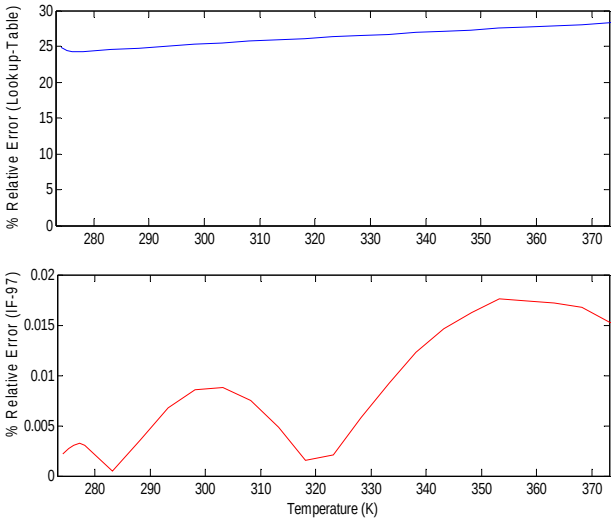

Figure 6: Specific entropy errors of the IF-97 and LUT models relative to the IAPWS95 standard

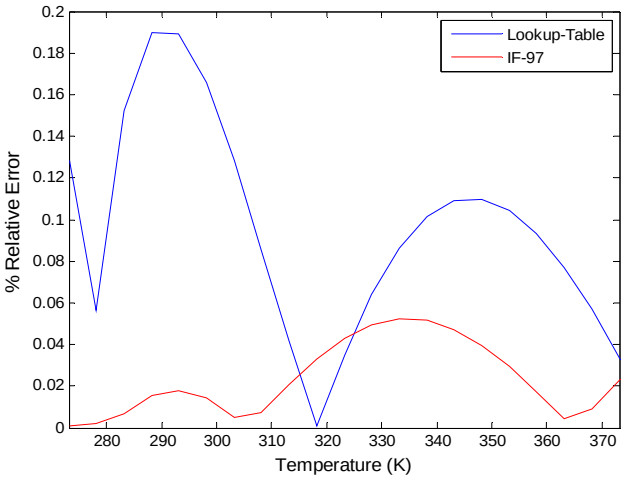

Figure 7: C_p errors of the IF-97 and LUT models relative to the IAPWS95 standard

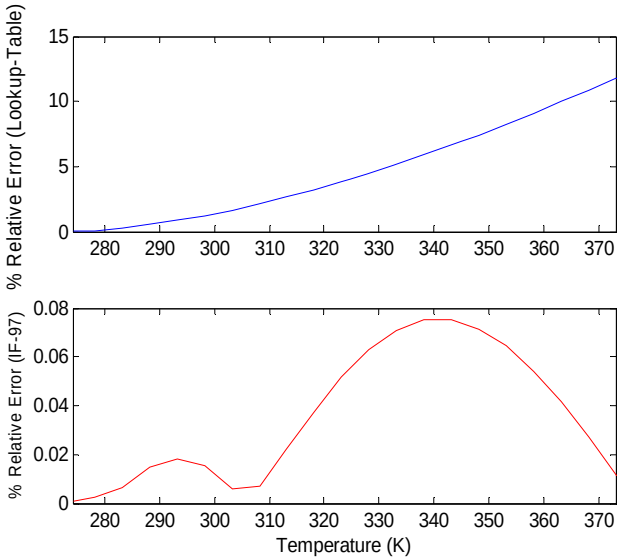

Figure 8: C_v errors of the IF-97 and LUT models relative to the IAPWS95 standard

Within the Modelica_Media Library, a group of *waterIF97* models have been well defined to compute the physical properties for water in the liquid, gas and two-phase regions based on the IF-97 formulae. However, there are several technical issues to use these *waterIF97* medium models directly in the functions of ACL. First, *waterIF97* medium model contains both single- and multiple-phase calculations, in which the multiple-phase portion is not needed for this application. In addition, earlier development in the ACL is well compatible with the automotive air conditioning systems whose working medium are various kinds of refrigerants. The composition is a critical argument contained in most functions developed in the ACL. For cooling and heating coils in the AHU, the single-phase water is the only working medium to deal with. The composition argument in the existing ACL functions results in significant inconvenience. For the single-phase water medium used in the heating/cooling coils, it would be more convenient to remove the composition argument.

Second, the medium property computation in the ACL covers both single- and multiple-phase processes, which are involved not only in the balance equations of the dynamic control volumes, but also in the calculations of various thermodynamic states, such as density, enthalpy and specific heats, which are irrelevant to the dynamic states of the control volumes. In addition, there are a lot of computations related to multiple-phase processes. A process/device involving only the single-phase water medium, such as the heating/cooling coil in the AHU, is a much simpler case. If we can remove all irrelevant computations, the resultant computational efficiency will be greatly improved.

Thirdly, the refrigerants used by typical automotive air conditioning systems are modeled on the basis of the Helmholtz functions with density-temperature as the pair of state variables. In many HVAC applications, it would be more convenient if the water properties are based on the pairs of pressure-temperature or pressure-enthalpy. In addition, for physical property calculations in the control volumes, the users can access the medium functions only at hierarchically higher levels, which limits the customization or reformulation of these functions for particular applications, especially when the user-preferred pair of state variables is not supported in the existing package.

To address the above issues, we decided to develop a simpler and more efficient water model, named as *CoolWater*, based on *Modelica_Media.Interfaces.PartialMedium*. The basic formulation of the *CoolWater* model was obtained from [35]. In particular, all redundant and conflicting variables and options in the original *waterIF97* model were either removed or modified, e.g. the BaseProperties code. To be consistent with the coding style and physical property calculations preserved in the ACL, several IF-97 based low-level medium functions and utilities were adopted from the Modelica_Media Library.

A heat exchanger model was developed based on the *CoolWater* medium described above. Heat exchanger modeling is generally considered the most computationally intensive entity in a refrigeration system [36]. To properly adapt the *CoolWater* model to the refrigerant side, equations in the dynamic control volumes should be rewritten, but the change should not degrade the overall inheritance structure and exactness of the heat exchanger model. Since the uppermost hierarchical structure of the heat exchanger is composed of only a few lines of code, the work of

implementing single-phase water model should begin from the most rudimentary control volumes. In the development phase, different choices of state-variable pairs were first compared and evaluated in order to achieve both engineering convenience and numerical efficiency. It was stated in [37] that the mass-internal-energy pair could decrease the numerical efficiency. The density-temperature pair was considered by [38] a bad choice in the liquid region for compressible fluids due to the amplification of numerical error.

Currently, the state-variable pairs of pressure-temperature and pressure-specific-enthalpy have been formulated into the heat exchanger model for comparison purpose. The techniques of state variable transformations were performed in the dynamic balance equations for pressure-temperature and pressure-specific-enthalpy, respectively [38, 39]. The corresponding partial derivatives appeared in the balance equations could be computed using rudimentary IF-97 functions. To ensure consistent and convenient initialization, the pressure-temperature pair (compared to the pressure-enthalpy pair) has been added into the initialization options, since temperature is easier to set for HVAC operation rather than some other variables such as enthalpy.

2.3.2 Validation of Cooling Coil Model

A cooling coil model was derived from the heat exchanger model described in the previous section. To validate this model, two comparisons were conducted: comparison of pressure-temperature and pressure-enthalpy and comparison of our cooling coil model and the cooling coil in ACL Version 1.5.

As described in [38], the advantage of using the pressure-temperature pair is that there are many medium property models which are explicit in this state pair. The sensitivity of using this state pair needs to be checked. It is known that using different dynamic state variable pairs may change the numerical sensitivity of the corresponding thermodynamic equations of state (EOS). For a bad choice of state pair, even a small error in one of variables of the state pairs may lead to a large error to other variables calculated from EOS. To address such concern, the pressure-temperature and pressure-enthalpy pairs were compared with an example cooling coil model.

The cooling coil adopted a flat tube louvered fin heat exchanger model given in the ACL. It consists of louvered fins and extruded microchannel flat tubes, both made of aluminum. The schematic diagrams in Figure 9 show the geometry and flow pattern for the cooling coil model.

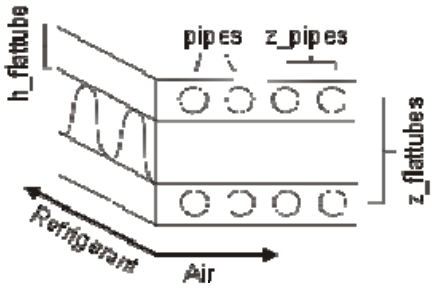

(a) Flow pattern of water and air

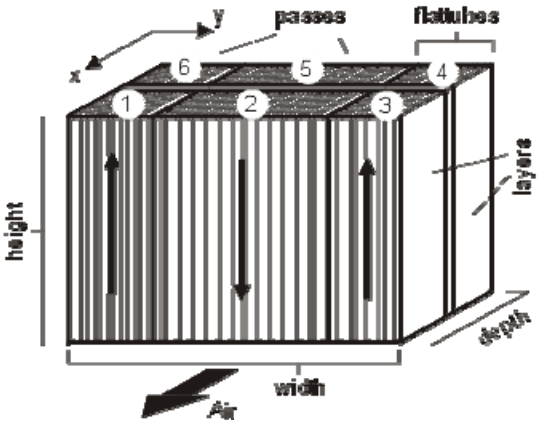

(b) Six-pass cooling coil with vertical flow of cooling water and cross flow of air

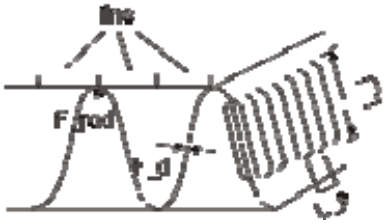

(c) Geometry of the triangular louvered fin

Figure 9: Schematic diagrams for the example cooling coil [40]

On both sides of the wall, several parallel flow channels are lumped into one uniform flow path. The cooling water path through the component is treated as one pipe flow with circular cross section and one air element associated with each flow segment. Each air element is further discretized along its flow direction. The total depth and height were set to be 0.06 m and 0.21 m, respectively. The width of the cooling coil could be then calculated from the known number of flat tubes and dimension of the flat tubes and fins. For the water side, as shown in Figure 9(b), there are 15 flat tubes in the 2nd and 5th flow passes, and 10 flat tubes in the each of the remaining flow passes. The dimension of the flat tubes could be determined through three parameters: height of one flat tube, center to center distance of two adjoining flat tubes, and the number of pipes in one flat tube. They were set to be 1 mm, 10 mm and 20, respectively. The

wall thickness and radius of each pipe were set to be 0.1 mm and 0.4 mm. At the air side, the shape of the louvered fins was set to be triangular. The fin dimensions are summarized in Table 2.

Table 2: Dimensions of the louvered fins

Fin Dimension	Parameter Setting
Number of fins per 0.1 m	80
Louver length (mm)	7
Louver pitch (mm)	1.4
Louver angle (°)	28
Fin thickness (mm)	0.1
Fin radius (mm)	0.4

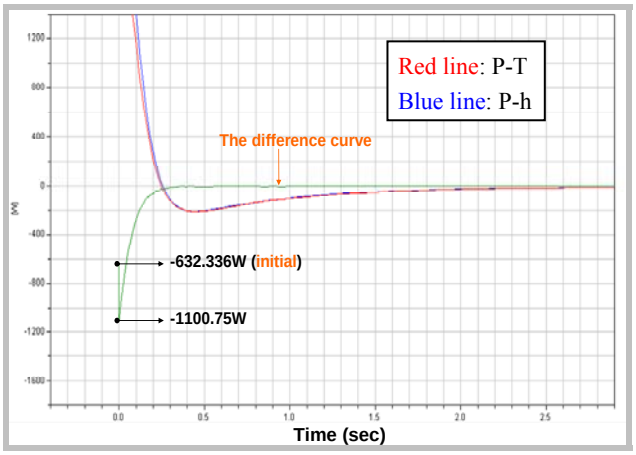

Figure 10: Internal energy in the 3rd control volume

For the two state pairs, the inlet air conditions were set identical. The flow rate, temperature and relative humidity of the inlet air were set to be 0.2 kg/s, 313K and 60%, respectively. For the water side, the chilled water flow rate was kept as 0.3 kg/s. For the pressure-temperature state pair, the initial temperature was set to 292.146 K. To be consistent with this setup, the inlet specific enthalpy was set to 8×10^4 kJ/kg for the pressure-enthalpy state pair. The total discretization number at the air side and water side was set to be 12 and 6, respectively. Figures 10 through 12 show the simulation results from our cooling performance test. The difference curves shown in the plots are the calculated numerical differences between these twos state variable pairs. The results indicate that the differences are noticeable only in the region of numerical transient responses, i.e. 0 to 0.5 seconds, which is not harmful to the overall transient and steady-state solutions.

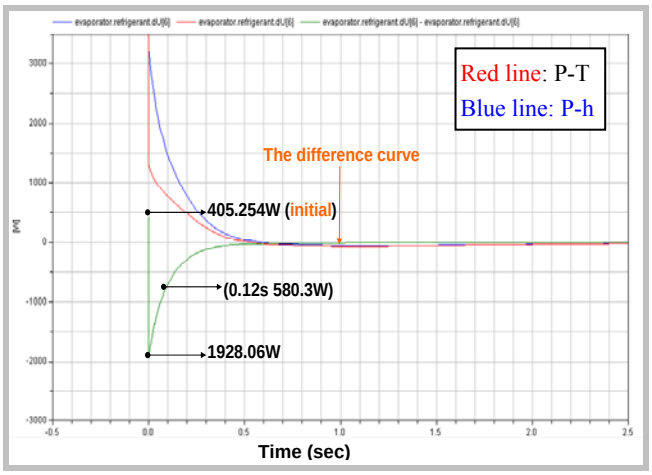

Figure 11: Internal energy in the 6th control volume

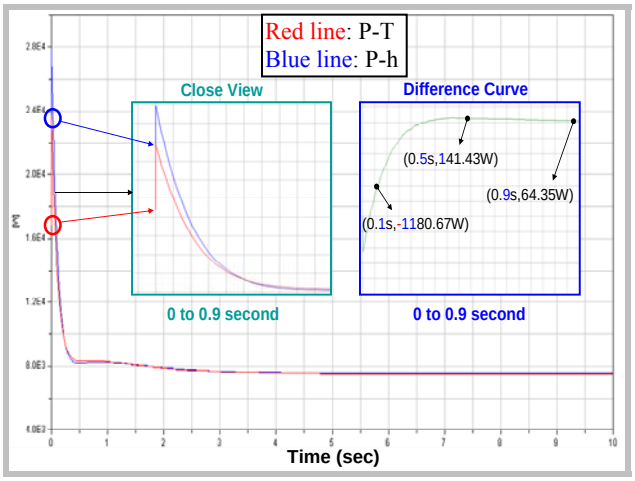

Figure 12: Total heat transferred from the heat exchanger

A further study was then performed to benchmark our development with the ACL Version 1.5. The heat exchanger model from ACL Version 1.5 was equipped with the LUT water model. In our case, the *CoolWater* model was used and pressure-temperature was selected as the state variable pair. The geometric configuration of the cooling coils was reinforced to be the same in the two cases. A similar cooling performance test was conducted, the initial air flow rate was 0.0675 kg/s and the air temperature and RH were given by 303.15 K and 60%, respectively. For the water side, the chilled water flow rate and initial temperature was kept as 0.1 kg/s and 293.15 K respectively. As shown in figure 13, the inlet temperatures at the water and the air sides respectively experienced ramp changes in sequence: at 30 second, the inlet water temperature first ramped to 298.15 K within 20 second, and then the inlet air temperature ramped to 308.15 K at 75 second within 20 second as well. Again, the total numbers of discretization at the air and water sides were set as 12

and 6, respectively. Figures 14 through 16 compare the simulation results of the two cases in terms of the specific enthalpy, the internal energy and the total heat transfer rate, respectively. The maximum relative error was found to be around 0.5%. For this single heat exchanger model test in our study, the computation time using the IF-97 model was about 50% more than that using the LUT model in the ACL Version 1.5.

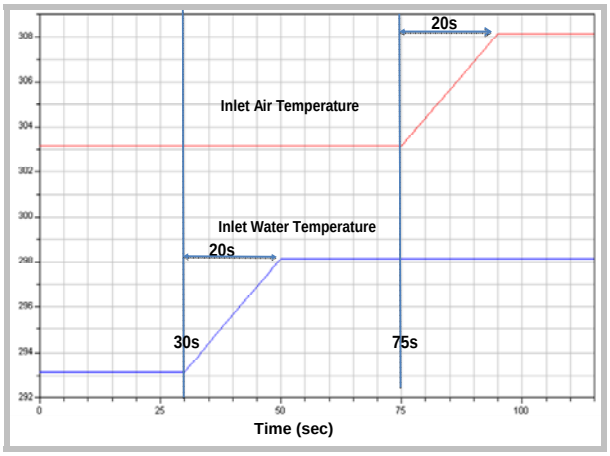

Figure 13: Sequential ramp changes of inlet water and air temperatures

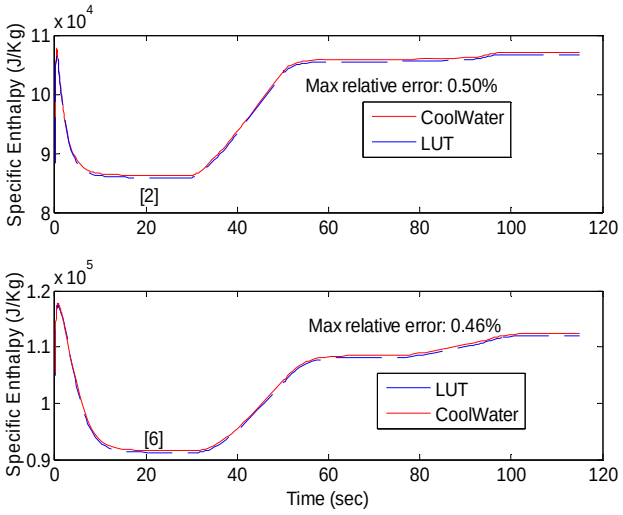

Figure 14: Specific enthalpy in the 2nd and 6th control volumes

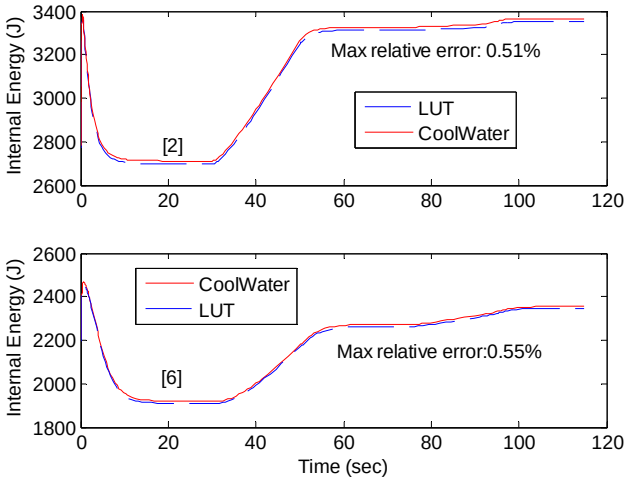

Figure 15: Internal Energy in the 2nd and 6th control volumes

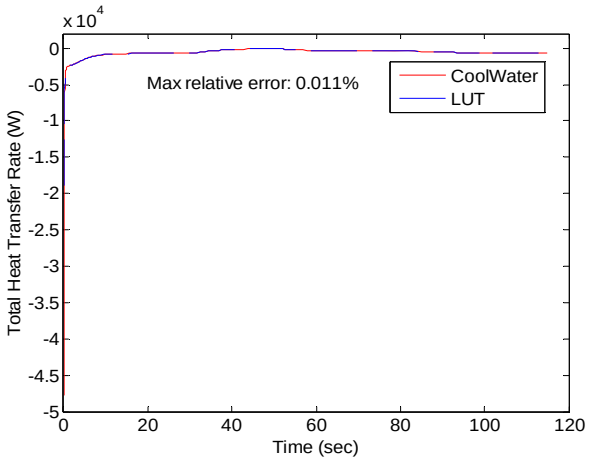

Figure 16: Total heat transfer rate at heat exchanger

3 Extremum Seeking Control (ESC) of Economizer Operation

3.1 Overview of ESC

The extremum seeking control deals with the on-line optimization problem of finding an optimizing input $u_{opt}(t)$ for the generally unknown and/or time-varying cost function $l(t, u)$, where $u(t) \in \mathbb{R}^m$ is the input parameter vector, i.e.

$$u_{opt}(t) = \arg\min_{u \in \mathbb{R}^m} l(t,u)\,. \qquad (3)$$

Figure 17 shows the block diagram for a typical ESC system [41]. The measurement of the cost function $l(t, u)$, denoted by $y(t)$, is corrupted by noise $n(t)$. The transfer function $F_I(s)$ denotes the linear dynamics of the mechanism that command the control or optimization parameter vector $u(t)$. $F_O(s)$ denotes the transfer function of the sensor dynamics that measure the

cost function, which is often a low-pass filter for removing noise from the measurement.

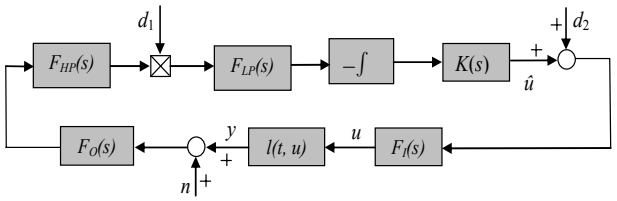

Fig. 17: Block diagram of extremum seeking control

The basic components of the ESC are defined as follows. The dithering and demodulating signals are denoted by $d_1^T(t) = \left[\sin(\omega_1 t) \quad \cdots \quad \sin(\omega_m t)\right]$ and $d_2^T(t) = \left[a_1 \sin(\omega_1 t) + \alpha_1 \quad \cdots \quad a_m \sin(\omega_m t) + \alpha_m\right]$, respectively, where ω_i are the dithering frequencies for each input parameter channel, and α_i are the phase angles introduced intentionally between the dithering and demodulating signals. The signal vector $d_2(t)$ contains the perturbation or dither signals used to extract the gradient of the cost function $l(t, u)$. These signals work in conjunction with the high-pass filter $F_{HP}(s)$, the demodulating signal $d_1^T(t) = \left[\sin(\omega_1 t) \quad \cdots \quad \sin(\omega_m t)\right]$ and the low-pass filter $F_{LP}(s)$, to produce a vector-valued signal proportional to the gradient $\frac{\partial l}{\partial u}(\hat{u})$ of the cost function at the input of the multivariable integrator, where $\hat{u}$ is the control input based on the gradient estimation. By integrating the gradient signal, asymptotic stability of the closed loop system will make the gradient vanish, i.e., achieving the optimality. Adding compensator $K(s)$ may enhance the transient performance by compensating the input/output dynamics. For a detailed explanation of ESC, consult references [12, 13, 41].

The earliest version of ESC can be dated back to Leblanc's work in 1922 [42]. There was great interest in this subject in 1950s and 1960's [10, 11, 43]. The research conducted by Krstić and his coworkers in the past decade ignited a resurgence of extremum-seeking control [12, 13]. Krstić and Wang first provided the stability proof for general SISO nonlinear plants based on averaging and singular perturbation methods [12]. More design issues were addressed in another paper by Krstić [13]. Later, the stability proof was extended to discrete-time situation [44]. The proposed ESC framework has been applied to various applications, such as maximizing biomass production rate [45], maximizing pressure rise in axial flow compressor [46], minimizing acoustic pressure oscillation to enhance combustion stability [47], minimizing the power demand in formation flight [48], and minimizing limit cycling [49], among others. The extremum seeking control was also studied along different paths. Özgüner and his coworkers combined ESC with sliding mode control [50-52] to study the vehicle ABS control. Based on the assumption of quadratic functional form with a finite number of parameters, Banavar developed an ESC scheme with an adaptation procedure of on-line identifying the parameters in the assumed function [53-55].

3.2 ESC for Energy Efficient Operation of Economizers

The ESC based economizer control is illustrated in Figure 18. The economizer control can be considered as a dual-loop structure. The inner loop is the supply air temperature control for the cooling coil, which has faster dynamics. The outer loop is the damper opening tuning for minimizing the cooling coil demand, which is realized with an ESC framework. The nonlinear performance mapping is from the outdoor air damper opening to the cooling coil demand, and the input dynamics are effectively the closed loop dynamics for supply air temperature control. In the three-state economizer operation scheme, as described in Section 1, the ESC is used for state 3 where mechanical cooling is required.

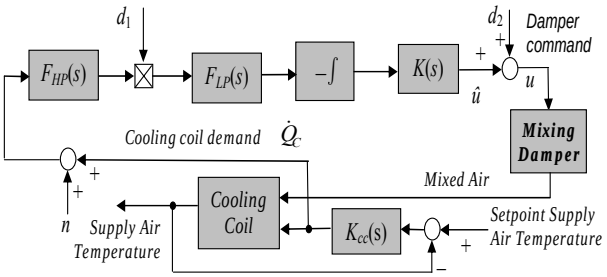

(a) Detailed block diagram

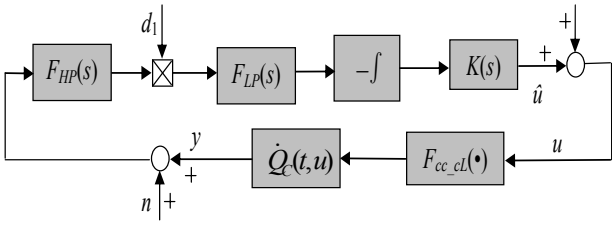

(b) Simplified block diagram

Figure 18: ESC based economizer control

3.3 Extremum Seeking Controller Design

Typical ESC design needs to determine the following parameters: the dither amplitude α, the dither frequency ω and phase angle ϕ, the high pass filter $F_{HP}(s)$, the low pass filter $F_{LP}(s)$, and the dynamic compensator $K(s)$. Based on averaging analysis, the

dither frequency should be relatively large with respective to the adaptation gain, but should not be too large to trigger unmodeled dynamics and make the system more sensitive to measurement noise. Also, if the dither frequency is well out of the bandwidth of the input dynamics, the roll-off in the magnitude response will slow down the convergence [13]. Therefore, dither frequency ω_d is typically chosen to be just a moderate value smaller than the cut-off frequency of the input dynamic as long as it is enough to separate the time scales of the dither signal and the inner loop dynamics. Generally, the dynamic compensator should be designed based on the dither signal, adaptation gain and the frequency responses of the input dynamics. Particularly, a proper proportional-derivative (PD) action can increase the phase margin of the input dynamics and thus make the inner loop more stable. However, extreme values of the adaptation gain, especially the derivative gain, will make the system unnecessarily affected by noise and thus destabilize the system. Further design guidelines are summarized as follows.

1) The dither frequency must be in the passband of the high pass filter and the stopband of the low pass filter, and it should be below the first cut-off frequency of the tuning schemes $F_I(s)$.
2) The dither amplitude should choose to be sufficiently small.
3) The dither phase angle should choose to satisfy $\theta = -\frac{\pi}{2} < \angle F_I(j\omega) + \alpha < \frac{\pi}{2}$ and it is desirable to design the phase angle $\theta = -\frac{\pi}{2} < \angle F_I(j\omega) + \alpha < \frac{\pi}{2}$ such that θ is close to zero.

3.4 Anti-windup ESC

Actuator saturation is often encountered in control systems. To our best knowledge, the issue of actuator saturation has not been discussed for extremum seeking control. For the economizer control, the actuator saturation will happen when it is cool or hot outside. For instance, when the outdoor air is around 53°F, the outdoor air damper will be positioned fully open to allow 100% outdoor air to enter the AHU. When it is warmer than 100 °F, the damper will be closed to a minimum opening which only maintain the lowest ventilation for indoor air quality [56]. In other words, the optimal reference input is not inside the saturation limit, but rather at either limit point. Transition between the ESC operation and the non-ESC operation is affected by the saturation issue. The averaging analysis of ESC [43] showed that, at a large time scale, the ESC can be deemed as a linear system regulating the gradient signal with a PI controller. When saturation presents in the ESC loop, integrator wind-up is unavoidable and, in consequence, leads to the undesirable windup phenomena. Later in Section 4.3, a simulation study will show that, due to the windup issue, the ESC action may be totally disabled even when the air condition changes to a point demanding its re-activation. It is thus necessary to modify the standard ESC structure in order to avoid integrator windup.

There has been much work reported in the field of anti-windup control (AWC) [57, 58]. In order to keep the simple nature of ESC, a back-calculation method is proposed as in Figure 19, following the spirit of the references [58-60]. The difference between the input and output of the actuator is fed back to the input end of the integrator through some gain factor. Our simulation results have demonstrated that this method works well to prevent the integrator windup in ESC system. Future research needs to investigate the design guidelines for the proposed anti-windup ESC. The analysis will be based on combining the existing method for back-calculation AWC and the averaging analysis [61, 62].

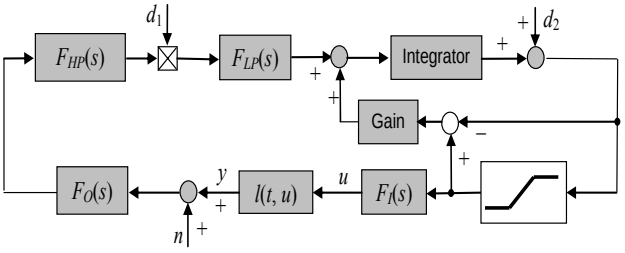

Figure 19: Block diagram for the anti-windup ESC

4 Simulation Study

The proposed extremum seeking control schemes were simulated with the Modelica based economizer model described in Section 2. The economizer model was used to identify the system dynamics and then illustrate the ESC schemes presented in the Section 3. At the point of writing this paper, the condensation computation from ACL 1.5 has not been incorporated into the cooling coil model due to the software licensing delay. Only the dry air can be simulated. The simulation results in the following are presented for illustration purpose. More rigorous treatment will be done after the condensation computation is made up to deal with moist air.

4.1 ESC with Standard Design

As previously stated, the control objective in this study is to minimize the chilled water flow rate of the cooling coil by tuning the OAD opening. The input dynamics from the OAD opening to the chilled

water flow rate was approximated based on several open-loop simulations. Fast (20 second) ramp input was used to approximate step input in order to remove the output jitter due to the inner loop PI control. Two fast-ramp responses are shown in Figure 20, which shows the second-order system behavior across the whole range of operating conditions.

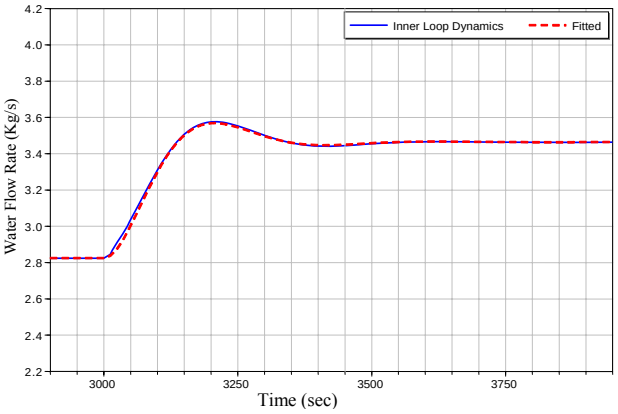

(a) Damper opening from 100% to 70%

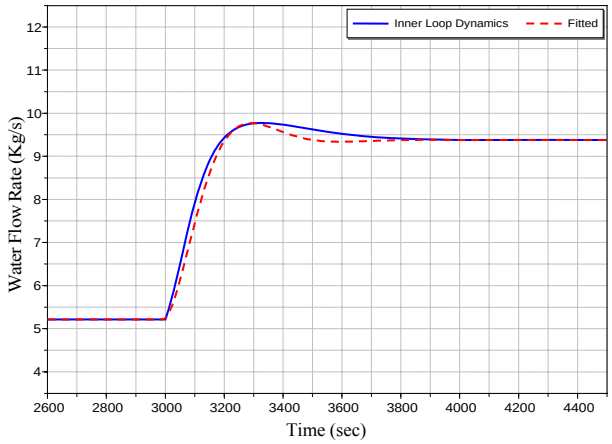

(b) Damper opening from 50% to 20%

Figure 20: Chilled water flow rate output under fast ramp change of outdoor air damper position

The following second order model was assumed to fit the fast-ramp test data:

$$F_I(s) = \frac{\omega_n^2}{s^2 + 2\zeta\omega_n s + \omega_n^2} \tag{4}$$

where ω_n is the undamped natural frequency and ζ is the damping ratio. The damping ratio ζ was first approximated by the percent overshoot suggested in [63], then the 10% to 90% rise time T_r was estimated. The ω_n can then be approximated via the following relationship with T_r and ζ [63]:

$$T_r = \frac{2.16\zeta + 0.60}{\omega_n} \tag{5}$$

which is accurate for $0.3 \le \zeta \le 0.8$.

A group of tests indicate that ω_n ranged from 0.0108 to 0.021 rad/sec. As a conservative approximation, ω_n was chosen to be 0.011 rad/sec. The damping ratio was estimated from the percent overshoot and was determined as 0.6. To properly separate the dither signal and plant dynamics, the dither frequency ω_d is selected as one tenth of the natural frequency. Next, the following high pass filter $F_{HP}(s)$ was selected:

$$F_{HP}(s) = \frac{s}{s + 0.0001} \tag{6}$$

which has a unit gain at the ω_d. The low pass filter was designed as

$$F_{LP}(s) = \frac{0.0006^2}{s^2 + 2 \cdot 0.6 \cdot 0.0006 s + 0.0006^2} \tag{7}$$

which has approximately 10dB and 20dB attenuation at ω_d and $2\omega_d$, respectively. To be consistent with the phase lag introduced by the input dynamics $F_I(s)$, the dither phase α was selected as 0.5π (radian), which makes $\theta = \angle F_I(j\omega) + \alpha \approx 0.1°$. The dither amplitude was chosen to be 10%.

The designed ESC was tested with a fixed operating condition. To be consistent with standard economizer design conditions, the supply air temperature is controlled at 55°F and the return air temperature is maintained around 75°F by providing a constant heat input to the indoor space. The system was started at minimal OAD opening (20%) to ensure adequate indoor air quality, and the ESC controller was turned on at about 3000 seconds to bring the system the optimum. The optimal OAD opening in this study is 100% since the outdoor air was set to 286K (55°F), which is always lower than the return air temperature 297K (75°F). Therefore, the more outdoor air intake, the less cooling water needed to be consumed. Figure 21 shows the time histories of the optimized chilled water flow rate and OAD opening. The obtained steady-state results are very close to the optimum since the assumed condition is mechanical cooling with optimal OAD opening at 100%.

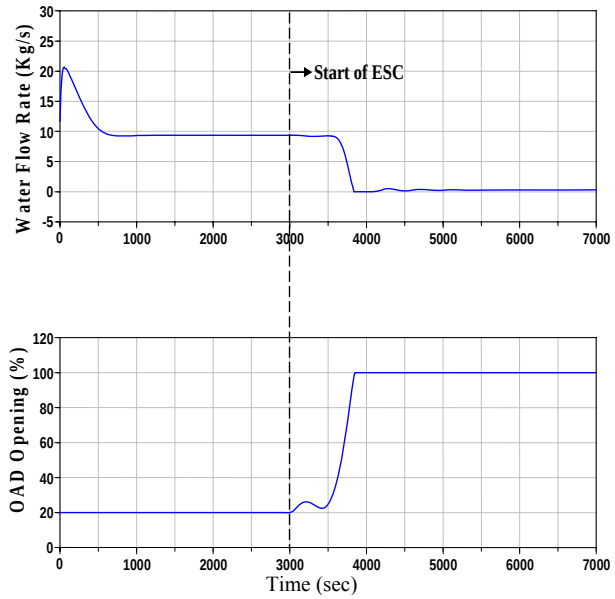

Figure 21: Tuning results of ESC with standard ESC.

4.2 Anti-Windup ESC

Another simulation study was conducted to verify the effectiveness of the proposed anti-windup ESC. Assume that a 20% damper opening is the minimum requirement for indoor air quality, and thus this was set as the lower saturation limit. The upper saturation limit was 100%. In the simulation study as shown in Figure 21, the initial outdoor air damper opening was set at 20%, the same as the lower saturation limit. The initial air temperature was again set to be 286 K. Figure 22 shows the integrator windup phenomenon when only the general ESC scheme was applied. Driven by the ESC, the damper opening was increased from 20% to 100% which was the corresponding achievable optimal setting. Then the outdoor air temperature was suddenly increased to 310 K (36.85 °C) at 6000 seconds, the new optimal opening was supposed to be below the lower saturation limit. However, the results show that the ESC was unable to respond to such change with reducing the damper opening. Rather the damper appeared "stuck" at the previous position. In comparison, as shown in Figure 23, applying the back-calculation based anti-windup ESC starting from 3000s effectively solved this problem. Therefore, the proposed anti-windup ESC scheme is shown to be able to handle the saturation windup problem.

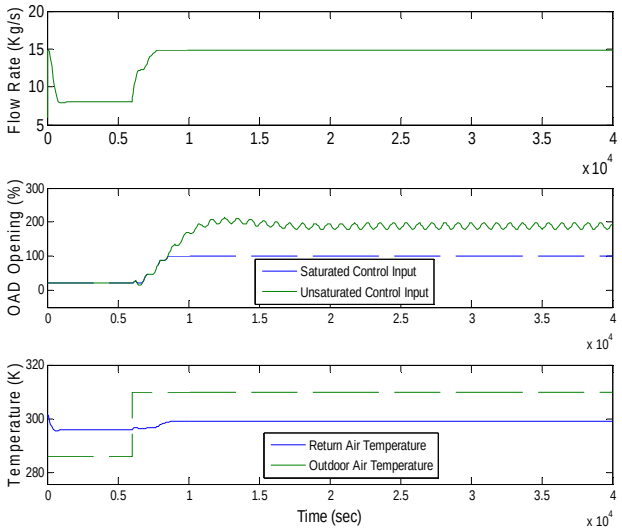

Figure 22: Standard ESC under actuator saturation

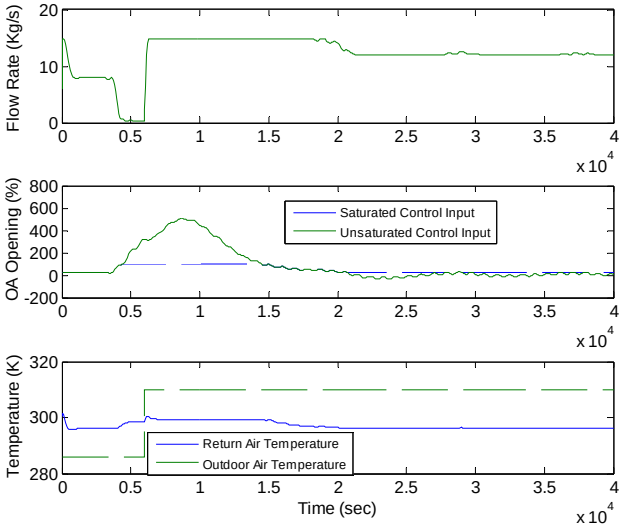

Fig. 23: Anti-windup ESC under damper saturation

5 Conclusions

In this paper, a Modelica based dynamic simulation model was developed for a single-duct air-side economizer based on Dymola and AirConditioning Library. In order to make the cooling coil modeling more effective and computationally efficient, revision was made on the water medium model and the associated heat exchanger modeling. An ESC algorithm was proposed as part of a three-state economizer operation, which aims to minimize mechanical cooling load for the economizer operation in commercial buildings. The standard ESC algorithm was enhanced by an anti-windup ESC scheme against damper (actuator) saturation. Simulations were conducted to search for the optimal outdoor air damper opening for standard ESC and the anti-windup ESC. The simulations results demonstrated the effective-

ness of using ESC for tuning the outdoor air damper position to minimize mechanical cooling load. The proposed enhancement was also validated through the simulation results.

References

1. EPA, *Energy Cost and IAQ Performance of Ventilation Systems and Controls*. EPA Report, 2000. **EPA-4-2-S-01-001**.
2. ASHRAE, *Energy Standard for Buildings Except Low-Rise Residential Buildings*. 2004, American Society of Heating, Refrigerating and Air-Conditiioning Engineers, Inc.: 1791 Tullie Circle NE, Atlanta, GA 30329.
3. ASHRAE, *90.1 User's Manual ANSI/ASHRAE/IESNA Standard 90.1-2004*. 2004, American Society of Heating, Refrigerating and Air-Conditioning Engineers, Inc.
4. Financial Times Energy, I. *Design Brief Economizers*.
5. NBCIP, *Product Testing Report: Duct-Mounted Relative Humidity Transmitters*. 2004, National Building Controls Information Program.
6. NBCIP, *Product Testing Report Supplement: Duct-Mounted Relative Humidity Transmitters*. 2005, National Building Controls Information Program.
7. Song, L. and M. Liu, *Optimal outside airflow control of an integrated air-handling unit system for large office buildings.* Journal of Solar Energy Engineering, Transactions of the ASME, 2004. **126**(1): p. 614-619.
8. Guo, C., Q. Song, and W. Cai, *A neural network assisted cascade control system for air handling unit.* IEEE Transactions on Industrial Electronics, 2007. **54**(1): p. 620-628.
9. Blackman, P.F., *Extremum-Seeking Regulators*, in *An Exposition of Adaptive Control*. 1962, Pergamon Press.
10. Sternby, J., *Extremum Control Systems: An Area for Adaptive Control?*, in *Preprints of the Joint American Control Conference*. 1980: San Francisco, CA.
11. Åström, K.J. and B. Wittenmark, *Adaptive control*. 2nd ed. 1995, Reading, Mass.: Addison-Wesley. xvi, 574 p.
12. Krstić, M. and H.-H. Wang, *Stability of extremum seeking feedback for general nonlinear dynamic systems.* Automatica, 2000. **36**(4): p. 595-601.
13. Krstić, M., *Performance improvement and limitations in extremum seeking control.* Systems and Control Letters, 2000. **39**(5): p. 313-326.
14. Bendapudi, S. and J.E. Braun, *A Review of Literature on Dynamic Models of Vapor Compression Equipment*. 2002.
15. Bourdouxhe, J.-P., M. Grodent, and J. Lebrun, *Reference Guide for Dynamic Models of HVAC Equipment*, ed. M. Geshwiler. 1998: American Society of Heating, Refrigerating & Air-Conditioning Engineers.
16. MacArthur, J.W. *Analytical Representation of the Transient Energy Interactions in Vapor Compression Heat Pumps*. 1984. ASHRAE, Atlanta, GA, USA.
17. MacArthur, J.W. and E.W. Grald, *Prediction of cyclic heat pump performance with a fully distributed model and a comparison with experimental data.* ASHRAE Transactions, 1987. **Vol. 93, Part 2**.
18. Nyers, J. and G. Stoyan, *Dynamical model adequate for controlling the evaporator of a heat pump.* International Journal of Refrigeration, 1994. **17**(2): p. 101-108.
19. Willatzen, M., N.B.O.L. Pettit, and L. Plough-Sorensen, *General dynamic simulation model for evaporators and condensers in refrigeration. Part I: Moving-boundary formulation of two-phase flows with heat exchange.* International Journal of Refrigeration, 1998. **21**(5): 398-403.
20. Rasmussen, B.P. and A.G. Alleyne, *Control-oriented modeling of transcritical vapor compression systems.* Journal of Dynamic Systems, Measurement and Control, Transactions of the ASME, 2004. **126**(1): 54-64.
21. Zhou, X., *Dynamic modeling of chilled water cooling coils*, in *School of Mechanical Engineering*. 2005, Purdue University.
22. Svensson, M.C., *Studies on on-line optimizing control with application to a heat pump*. 1994, The University of Trondheim.
23. He, X., S. Liu, and H. Asada. *Modeling of vapor compression cycles for advanced controls in HVAC systems*. 1995. Seattle, WA, USA.
24. Wang, S., J. Wang, and J. Burnett, *Mechanistic model of centrifugal chillers for HVAC system dynamics simulation.* Building Services Engineering Research and Technology, 2000. **21**(2): p. 73-83.
25. Modelica. 2007 [cited; Available from: http://www.modelica.org/.
26. Modelon. 2007 [cited; Available from: http://www.modelon.se/.
27. Videla, J.I. and B. Lie. *A New Energy Building Simulation Library*. in *Proceedings of Modelica 2006*. 2006.
28. Dynasim. http://www.dynasim.se/dynasim.htm.

29. Lebrun, J., *Variable Speed Fan*, http://cbs.lbl.gov/diagnostics/model_library. 2004.
30. Wagner, W., et al., *The IAPWS industrial formulation 1997 for the thermodynamic properties of water and steam.* Journal of Engineering for Gas Turbines and Power, 2000. **122**(1): p. 150-180.
31. Tan, H. and A. Dexter, *Estimating airflow rates in air-handling units from actuator control signals.* Building and Environment, 2006. **41**(10): p. 1291-1298.
32. Limperich, D., et al. *System Simulation of Automotive Refrigeration Cycles*. in *Proceedings of the 4th International Modelica Conference*. 2005. Hamburg.
33. Wagner, W. and A. Pruß, *The IAPWS Formulation 1995 for the Thermodynamic Properties of Ordinary Water Substance for General and Scientific Use.* J. Phys. Chem. Ref. Data 2002. **Volume 31**(Issue 2): p. 387-535.
34. Wagner, D.-I.W. and D.-I.U. Overhoff, *FLUIDCAL*. 2004. Basic Package Water (IAPWS-95) for calculating the thermodynamic properties of H_2O.
35. Hilding Elmqvist, H.T.a.M.O. *Object-Oriented Modeling of Thermo-Fluid Systems*. in *Proceedings of the 3rd International Modelica Conference*. 2003. Linköping.
36. Bendapudi, S., *Development and evaluation of modeling approaches for transients in centrifugal chillers*. 2004, Purdue University
37. Torge Pfafferott, G.S. *Implementation of a Modelica Library for Simulation of Refrigeration Systems*. *Proceedings of the 3rd International Modelica Conference*. 2003. Linköping.
38. Tummescheit, H., *Design and Implementation of Object-Oriented Model Libraries using Modelica*, in *Department of Automatic control*. 2002, Lund Institute of Technology.
39. Eborn, J., *On Model Libraries for Thermohydraulic Applications*, *Department of Automatic Control*. 2001. Lund Inst. of Technology.
40. Modelon AB, *AirConditioning Library Users Mannaul Version 1.5*. 2007.
41. Rotea, M.A., *Analysis of multivariable Extremum Seeking Algorithms.* Proceedings of the American Control Conference, 2000. p. 433-437
42. Leblanc, M., *Sur l'electrification des Chemins de fer au Moyen de Courants Alternatifs de Frequence Elevee.* Revue Generale de l'Electricite, 1922.
43. Tsien, H.S., *Engineering cybernetics*. 1954, New York,: McGraw-Hill. xii, 289p.
44. Choi, J.Y., et al., *Extremum seeking control for discrete-time systems.* IEEE Transactions on Automatic Control, 2002. **47**(2): p. 318-323.
45. Wang, H.H., M. Krstic, and G. Bastin, *Optimizing bioreactors by extremum seeking.* International Journal of Adaptive Control and Signal Processing, 1999. **13**(8): p. 651-669.
46. Wang, H.-H., S. Yeung, and M. Krstic, *Experimental application of extremum seeking on an axial-flow compressor.* IEEE Transactions on Control Systems Technology, 2000. **8**(2): p. 300-309.
47. Banaszuk, A., Y. Zhang, and C.A. Jacobson. *Adaptive control of combustion instability using extremum-seeking*. in *Proceedings of the American Control Conference*. 2000.
48. Binetti, P., et al., *Control of formation flight via extremum seeking.* Proceedings of the American Control Conference, 2002. **4**: p. 2848-2853.
49. Wang, H.-H. and M. Krstić, *Extremum seeking for limit cycle minimization.* IEEE Transactions on Automatic Control, 2000. **45**(12): p. 2432-2437.
50. Drakunov, S., et al., *ABS control using optimum search via sliding modes.* IEEE Transactions on Control Systems Technology, 1995. **3**(1): p. 79-85.
51. Yu, H. and Ü. Özgüner. *Extremum-seeking control strategy for ABS system with time delay*. in *Proceedings of the American Control Conference*. 2002.
52. Yu, H. and Ü. Özgüner. *Extremum-seeking control via sliding mode with periodic search signals*. in *Proceedings of the IEEE Conference on Decision and Control*. 2002.
53. Speyer, J.L., et al. *Extremum seeking loops with assumed functions*. in *Proceedings of the IEEE Conference on Decision and Control*. 2000.
54. Banavar, R.N., D.F. Chichka, and J.L. Speyer. *Functional feedback in an extremum seeking loop*. in *Proceedings of the IEEE Conference on Decision and Control*. 2001.
55. Banavar, R.N. *Extremum seeking loops with assumed functions: Estimation and control*. in *Proceedings of the American Control Conference*. 2002.
56. ASHRAE, *ASHRAE standard : ventilation for acceptable indoor air quality*. 2001, Atlanta, GA: American Society of Heating, Refrigerating and Air-Conditioning Engineers, Inc. 34 p.
57. Åström, K.J. and B. Wittenmark, *Computer-Controlled Systems: Theory and Design*. 3rd ed. Prentice Hall information and system sciences series. 1997, Upper Saddle River, N.J.: Prentice Hall. xiv, 557 p.

58. Åström, K.J. and L. Rundqwist. *Integrator windup and how to avoid it*. in *Proceedings of 1989 American Control Conference*. 1989.
59. Fertik, H.A. and C.W. Ross, *Direct digital control algorithms with anti-windup feature.* ISA Transactions, 1967: p. 317-328.
60. Åström, K.J., *Advanced control methods – Survey and assessment of possibilities*, in *Advanced control in computer integrated manufacturing. Proceedings of the thirteenth annual Advanced Control Conference* H.M. Morris, E.J. Kompass, and T.J. Williams, Editors. 1987.
61. Sanders, J.A., F. Verhulst, and J.A. Murdock, *Averaging methods in nonlinear dynamical systems*. 2nd ed. 2007, New York: Springer.
62. Khalil, H.K., *Nonlinear systems*. 3rd ed. 2002, Upper Saddle River, N.J.: Prentice Hall.
63. Dorf, R.C. and R.H. Bishop, *Modern Control Systems (10th Edition)*. 2004: Prentice Hall.
64. DOD, *Heating, Ventilating, Air Conditioning, and Dehumidfying Systems*. 2005, United States Department of Defense.
65. Hydeman, M., et al., *Advanced Variable Air Volume System Design Guide*. 2003, California Energy Commission.

Appendix: Economizer Operation

The American Society of Heating, Refrigerating and Air Conditioning Engineers (ASHRAE) recommends using economizers based on the cooling capacity size and weather characteristics for the building location. ASHRAE [2] classifies climate data based on temperature with a number from 1 to 7, and the letters A, B, and C, which correspond to moist, dry, and marine climates, respectively. Table 1 contains climate zones for 16 cities in the United States. The fourth column (Economizer Requirement) shows the cooling capacity for which an economizer is required by ASHRAE [2]. No economizer is required in weather locations 1A, 1B, 2A, 3A, and 4A. In weather locations 3B, 3C, 4B, 4C, 5B, 5C, and 6B, an economizer is required when the cooling requirement is greater than or equal to 19 kW. In all other weather locations, an economizer is required when the cooling requirement is greater than or equal to 40 kW. ASHRAE [3] describes several control strategies for transitioning between 100% outdoor air and the minimum outdoor air required for ventilation. The control strategies are called “high limit shutoff control for air economizer.” Following is a list of strategies that can be programmed in a computer control system.

- *Fixed dry bulb temperature*. This strategy compares the outdoor temperature to a transition temperature. If the outdoor air temperature is greater than the transition temperature, then the dampers are controlled for the minimum outdoor air required for ventilation. ASHRAE [3] said this is the most reliable and simple control strategy since a simple thermostat placed in an outdoor air intake can be used. Table 2 shows the transition temperature for different climatic zones. The U.S. Department of Defense [64] recommends this strategy.
- *Differential dry bulb temperature*. This control strategy compares the outdoor and return air temperatures. If the outdoor temperature is greater than the return air temperature, then the dampers are controlled for minimum outdoor air required for ventilation. This strategy should not be used in the following climatic zones: 1A, 2A, 3A, and 4A. Hydeman et al. [65] said, "Of all of the options, dry bulb temperature controls prove the most robust as dry-bulb temperature sensors are easy to calibrate and do not drift excessively over time. Differential control is recommended throughout California and the sensors should be selected for a through system resolution of 0.5 °F. Dry-bulb sensors work well in all but humid climates, which are not typical in California."
- *Fixed enthalpy*. This control strategy measures the outdoor air temperature and relative humidity. Then the outdoor air enthalpy is calculated and compared with a transition enthalpy. If the outdoor air enthalpy is greater than the transition enthalpy, then the dampers are controlled for minimum outdoor air required for ventilation. ASHRAE [2] recommends a transition enthalpy of 47kJ/kg and at locations with altitudes significantly different than sea level, the transition enthalpy should be determined for 24 °C and 50% relative humidity. This strategy should not be used in the following climatic zones: 1B, 2B, 3B, 3C, 4B, 4C, 5B, 5C, 6B, 7, and 8, due to the problem with humidity sensors.
- *Differential enthalpy*. This control strategy determines the outdoor and return air enthalpy from measurements of the outdoor and return air temperature and relative humidity. If the outdoor air enthalpy is greater than the return air enthalpy, then the dampers are controlled for minimum outdoor air required for ventilation. In 2003, the U.S. General Services Administration required a differential enthalpy economizer for air-handling units with a capacity greater than 3,000 CFM (1,416 LPS) unless the air handling system design precluded the use of an air-side economizer. Regarding the use of differential enthalpy controls, Hy-

deman et al. [65] said, "Differential enthalpy controls are theoretically the most energy efficient. The problem with them is that the sensors are very hard to keep calibrated and should be re-calibrated on an annual or semi-annual basis. Contrary to common perception, enthalpy controls do not work in all climates. In hot dry climates they can hunt and excessively cycle the economizer dampers when the hot dry outdoor air has lower enthalpy than the space(s) at cooling balance point. What happens is that the economizer opens up and the coil is dry, which in turn dries out the space(s) until the return enthalpy goes below the outdoor enthalpy. As a result, the economizer damper closes, the space humidity increases, and the cycle repeats."

Table A.1. Climate zones and economizer requirement for 16 US cities. (q_{cool}: cooling capacity)

Climate	Description	Cities	Economizer Requirement
1A	Very Hot - Humid	Miami, FL	None
1B	Very Hot - Dry	---	None
2A	Hot - Humid	Houston, TX	None
2B	Hot - Dry	Phoenix, AZ	$q_{cool} \geq 40$ kW
3A	Warm - Humid	Charlotte, NC	None
3B	Warm - Dry	Los Angeles, CA	$q_{cool} \geq 19$ kW
3C	Warm - Marine	San Francisco, CA	$q_{cool} \geq 19$ kW
4A	Mixed - Humid	New York, NY	None
4B	Mixed - Dry	Albuquerque, NM	$q_{cool} \geq 19$ kW
4C	Mixed - Marine	Seattle, WA	$q_{cool} \geq 19$ kW
5A	Cool - Humid	Chicago, IL	$q_{cool} \geq 40$ kW
5B	Cool - Dry	Denver, CO	$q_{cool} \geq 19$ kW
5C	Cool - Marine	---	$q_{cool} \geq 19$ kW
6A	Cold - Humid	Minneapolis, MN	$q_{cool} \geq 40$ kW
6B	Cold - Dry	Cheyenne, WY	$q_{cool} \geq 19$ kW
7A	Very Cold - Humid	Ashland, WI	$q_{cool} \geq 40$ kW
7B	Very Cold - Dry	Jackson, WY	$q_{cool} \geq 40$ kW
8	Arctic	Fairbanks, AL	$q_{cool} \geq 40$ kW

Table A.2. Transition temperatures for fixed dry bulb economizer.

Climatic Zones	Transition Equation
1B, 2B, 3B, 4B, 4C, 5B, 5C, 6B, 7B, 8	$T_{OA} > 24^{\circ}\mathrm{C}$
5A, 6A, 7A	$T_{OA} > 21^{\circ}\mathrm{C}$
1A, 2A, 3A, 4A	$T_{OA} > 18^{\circ}\mathrm{C}$